Planet. Space Sci., Vol. 36, No. 3, pp. 271–279, 1988
Printed in Great Britain.

0032-0633/88 $3.00 + 0.00

THE ROLE OF NITRIC OXIDE ON THE ZONALLY AVERAGED STRUCTURE OF THE THERMOSPHERE: SOLSTICE CONDITIONS FOR SOLAR CYCLE MAXIMUM

J.-CL. GÉRARD
Institut d'Astrophysique, Université de Liège, 4200 Cointe-Liège, Belgium

and

R. G. ROBLE
High Altitude Observatory, National Center for Atmospheric Research,* P.O. Box 3000, Boulder, CO 80307, U.S.A.

(*Received* 24 *September* 1987)

Abstract—A zonally averaged chemical-dynamical model of the Earth's thermosphere is used to examine the importance of nitric oxide 5.3 μm cooling in controlling the dynamic structure of the thermosphere for December solstice during solar maximum ($F_{10.7} = 200 \times 10^{-22}$ W m^{-2} Hz^{-1}, $A_p = 10$). A previous study (Gérard and Roble, 1986, *Planet. Space Sci.* **34**, 131) showed that NO cooling was generally small for solar cycle minimum because of low NO densities and low thermospheric temperatures. Nevertheless, NO 5.3 μm cooling was sufficient to weaken the summer-to-winter pole temperature difference by about 45 K with an 8 m s^{-1} reduction in the zonally averaged meridional wind velocity. For solar cycle maximum conditions considered in this study, the effect of NO 5.3 μm cooling is larger because of enhanced NO densities and larger thermospheric temperatures. NO cooling reduces the summer-to-winter pole temperature difference by 110 K with a 25 m s^{-1} reduction in the zonally averaged meridional wind velocity. There are correspondingly larger changes in the mean compositional structure of the thermosphere for solar maximum compared to solar minimum. These results show that it is important to consider the heating and cooling effects of the minor neutral constituents, NO, N(^{4}S) and N(^{2}D) when calculating the circulation, temperature and compositional structure of the thermosphere.

1. INTRODUCTION

In a previous paper, Gérard and Roble (1986) [hereafter referred to as Paper I], we used a coupled zonally-averaged chemical-dynamical model of the Earth's thermosphere to investigate the importance of nitric oxide 5.3 μm cooling in controlling the dynamic structure of the thermosphere for solstice conditions during solar cycle minimum. The results of that study showed that the primary effect of the 5.3 μm cooling is to weaken the summer-to-winter latitudinal temperature gradient and the summer-to-winter mean meridional circulation. In the upper thermosphere, NO 5.3 μm cooling reduced the summer-to-winter pole temperature difference by about 45 K with an 8 m s^{-1} reduction in the zonally averaged meridional wind velocity. There were corresponding reductions in the vertical and mean zonal wind velocities and changes in composition of about -40% for O_2 and $+15\%$ for O in the upper thermosphere at high summer latitudes. The overall effect of NO cooling on the dynamic structure of the thermosphere was generally small for solar cycle minimum. This conclusion is consistent with that made in a previous study by Roble and Emery (1983) who examined the role of NO cooling on the global mean structure of the thermosphere. The low NO densities and low thermospheric temperatures produced a relatively small amount of NO 5.3 μm radiational cooling during solar minimum. For solar maximum, however, NO cooling was expected to be larger because of the increased NO densities and thermospheric temperatures. In this paper, we present results of a study similar to that of Paper I but for solar cycle maximum conditions. The results show that NO 5.3 μm cooling has a greater effect in establishing the basic thermospheric structure for solstice conditions during solar cycle maximum.

2. MODEL

The model used to calculate the zonally averaged circulation, temperature and compositional structure of

* The National Center for Atmospheric Research is sponsored by the National Science Foundation.

the thermosphere for December solstice during solar maximum is the same as that described by Gérard and Roble (1986). That model was based on previous studies by Kasting and Roble (1981), Roble and Kasting (1984) and Gérard *et al.* (1984). The formulation of NO cooling by Kockarts (1980) is used to calculate the thermospheric cooling rate per unit mass.

The major modifications to the model from that described in Paper I are the following.

(1) Neutral gas heating rates and O_2 photodissociation rates are determined using solar maximum e.u.v. and u.v. fluxes given by Torr and Torr (1985) and Rottman (1981) respectively and linearly extrapolated to correspond to a $F_{10.7}$ solar index of 200×10^{-22} W m^{-2} Hz^{-1}. The contribution of the Schumann–Runge continuum is calculated from the parameterization by Torr *et al.* (1980) normalized to the u.v. flux measured by Rottman (1981).

(2) The electron densities for solar maximum are calculated using the specified solar flux values and are used to derive the ion drag parameters for the model.

(3) The auroral particle source is the same as that used in Paper I to model solar minimum geomagnetically quiet conditions [case (b) described by Gérard *et al.*, 1984]. The Joule heat source Q_J is determined by specifying a high latitude distribution of electric field, E, and using the calculated electron densities to determine the Pedersen conductivity, σ_p,

$$Q_J = \sigma_p E^2.$$

The integrated Joule heating rate is 1×10^{11} W, a value larger than the heat input used in Paper I, the consequence of increased conductivities at solar maximum.

Starting from the solar minimum solution, the coupled model is run to steady state, using the solar maximum input fields. The model calculates the perturbation temperature about a global mean reference profile obtained from the MSIS-83 (Hedin, 1983) empirical model for solar cycle maximum and which is shown in Fig. 1. It corresponds to values of $F_{10.7} = 200$ and $A_p = 10$. The exospheric temperature is 1250 K. Below 85 km, the temperature profile is identical to that adopted by Kasting and Roble (1981) and the N_2 and O_2 densities are extrapolated downward assuming hydrostatic equilibrium.

3. RESULTS

As in Paper I, two identical model runs were made: one including NO 5.3 μm cooling and the other not.

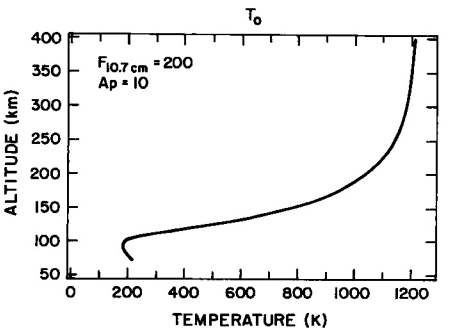

FIG. 1. GLOBAL MEAN TEMPERATURE VERTICAL STRUCTURE FOR SOLAR MAXIMUM CONDITIONS ($F_{10.7} = 200 \times 10^{-22}$ W m^{-2} Hz^{-1}) AND QUIET GEOMAGNETIC CONDITIONS ($A_p = 10$) AS OBTAINED FROM THE MSIS-83 EMPIRICAL MODEL OF TEMPERATURE AND COMPOSITION.

The model solutions for the case with NO 5.3 μm cooling are presented and the differences between the two model runs are presented as difference fields. The model solutions with NO 5.3 μm cooling are also compared with zonally averaged temperature, N_2, O_2 and O density distributions obtained from the mass spectrometer and incoherent scatter empirical model of Hedin (1983) for similar geophysical conditions.

3.1. *Total fields with* NO *cooling*

The calculated zonally averaged neutral temperature distribution for December solstice conditions for solar maximum is shown in Fig. 2a. There is about a 400 K exospheric temperature difference between the summer and winter poles. During solar minimum, the summer-to-winter pole exospheric temperature difference was 170 K as shown in Fig. 1c of Paper I. In the lower thermosphere, the temperature gradients are considerably weaker than that at exospheric heights. The calculated zonally averaged meridional winds are shown in Fig. 2b. There is a general flow from the summer-to-winter hemisphere at all levels except for the region between 150 and 200 km where there is a weak return thermospheric circulation from the winter-to-summer hemisphere. Maximum wind speeds of 70 m s^{-1} occur near 60° latitude in the summer hemisphere with a secondary maximum of 60 m s^{-1} near 30° latitude in the winter hemisphere. For solar minimum the maximum wind speed in the summer hemisphere is 30 m s^{-1} with a weak reverse circulation developing in the winter hemisphere as a result of high latitude heating as shown in Fig. 1a of Paper I. The reverse high latitude circulation does not develop for solar maximum because of the stronger solar forcings.

The zonal wind velocities are westward in the summer hemisphere at about 10 m s^{-1} and eastward in

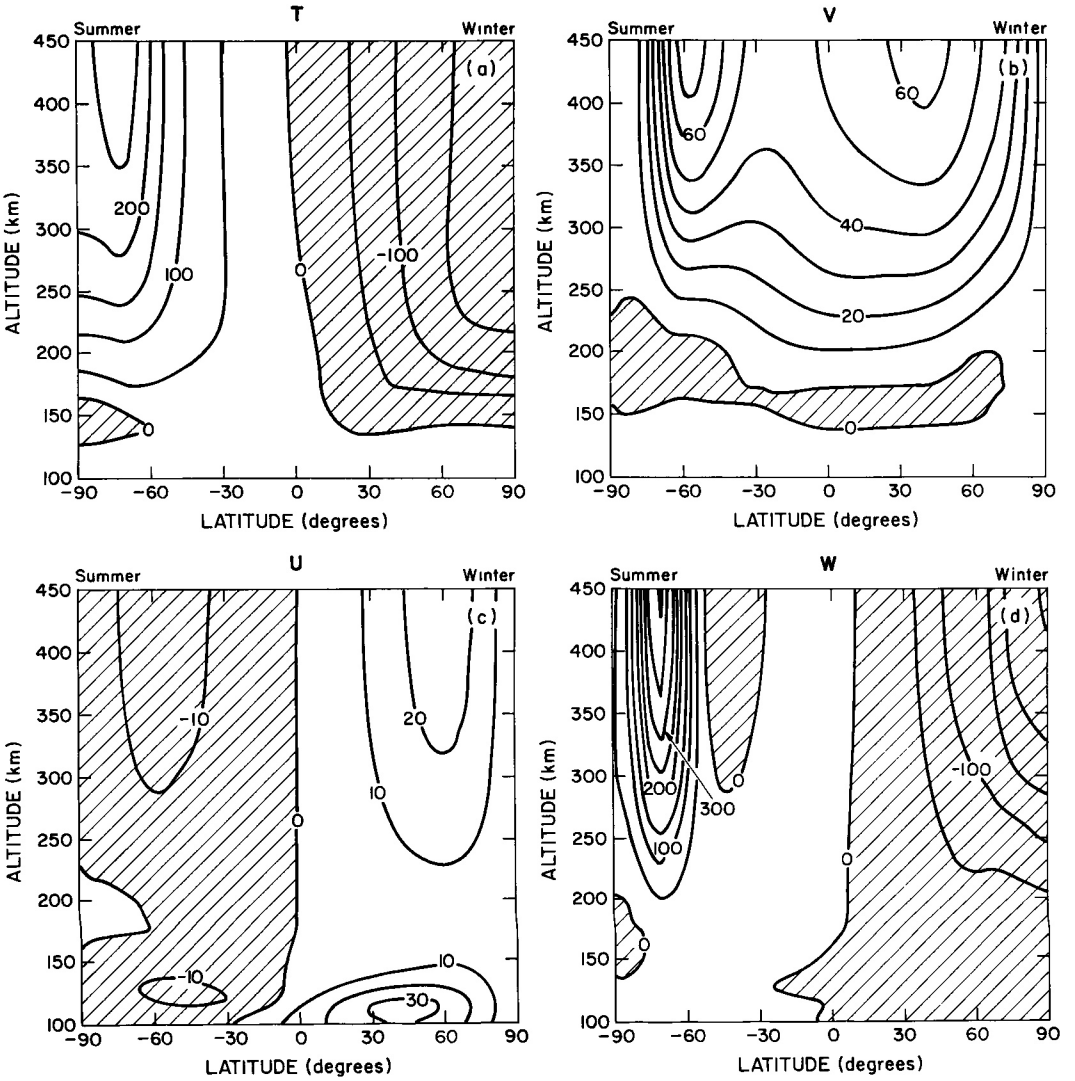

FIG. 2. (a) CALCULATED ZONALLY AVERAGED NEUTRAL PERTURBATION TEMPERATURE, FROM THE GLOBAL MEAN STRUCTURE SHOWN IN FIG. 1, IN K FOR DECEMBER SOLSTICE AND SOLAR CYCLE MAXIMUM CONDITIONS FOR THE CASE WHEN NO COOLING IS INCLUDED, (b) ZONALLY AVERAGED MERIDIONAL WIND (m s^{-1}, POSITIVE NORTHWARD), (c) ZONALLY AVERAGED ZONAL WIND (m s^{-1}, POSITIVE EASTWARD), (d) ZONALLY AVERAGED VERTICAL WIND (cm s^{-1}, POSITIVE UPWARD).

the winter hemisphere as shown in Fig. 2c. These solar driven wind velocities are weak and of comparable magnitude to those calculated for solar minimum as shown in Fig. 1b of Paper I. There is no specified zonal mean momentum source caused by the correlation of diurnal winds and ion drag as considered by Dickinson *et al.* (1975) in these calculations.

The vertical winds are upward in the summer hemisphere and downward in the winter hemisphere as shown in Fig. 2d. A maximum upward wind of about 4 m s^{-1} occurs in the summer auroral zone and downward motion exists throughout the winter hemisphere. For solar minimum conditions there was weak upward motion in the high latitude winter hemisphere. These differences are a consequence of weaker auroral heating and stronger solar forcing in the winter hemisphere during solar maximum.

The N_2, O_2 and O distributions for this case are shown in Figs 3a, 3b and 3c, respectively. The molecular species N_2 and O_2 are enhanced in the summer

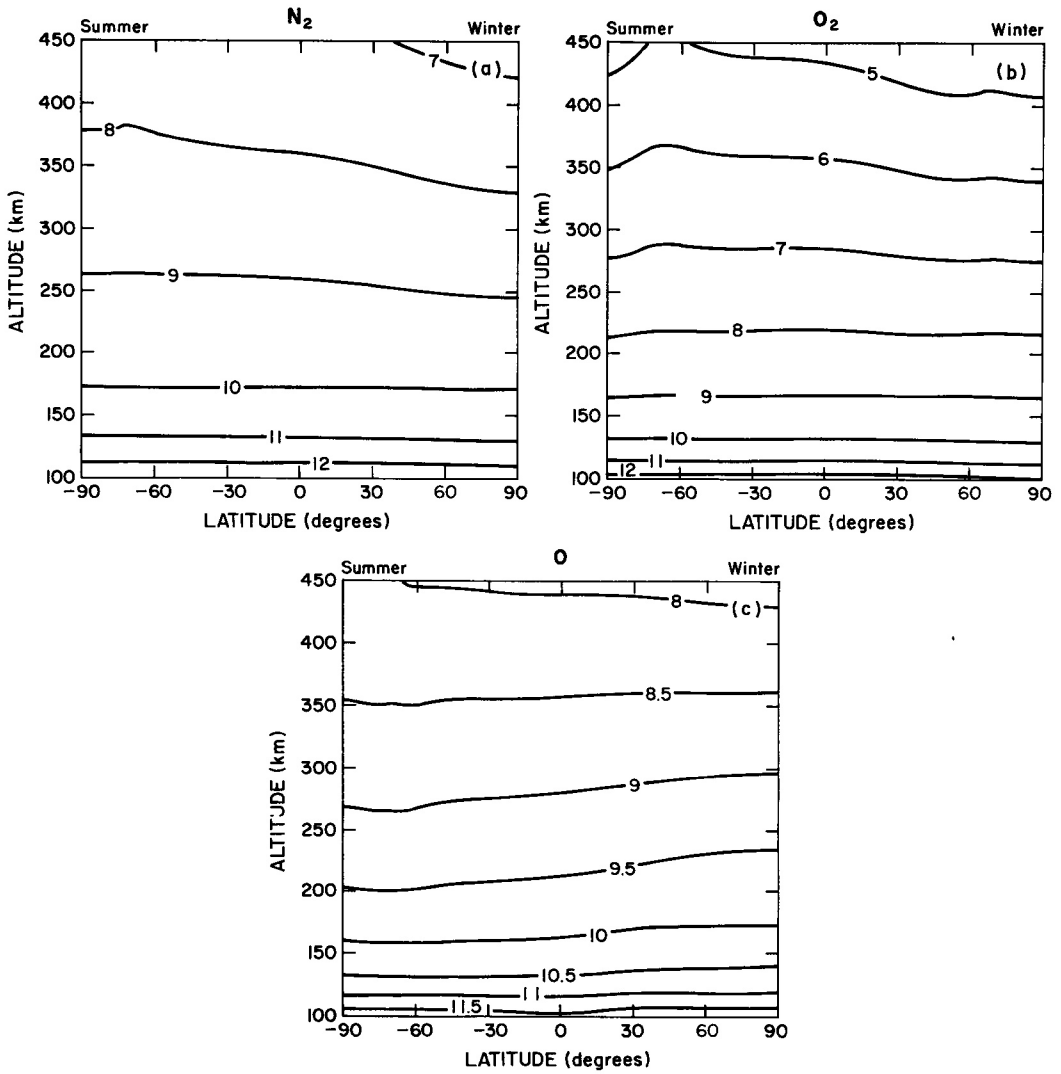

FIG. 3. CALCULATED ZONALLY AVERAGED DISTRIBUTION OF THE LOG_{10} (a) N_2, (b) O_2 AND (c) O NUMBER DENSITIES (cm^{-3}) FOR DECEMBER SOLSTICE AND SOLAR CYCLE MAXIMUM CONDITIONS FOR THE CASE WHEN NO COOLING IS INCLUDED.

hemisphere and atomic oxygen is enhanced in the winter hemisphere similar to the distributions shown in Fig. 2 of Paper I. There are, however, stronger O_2 and N_2 enhancements in the auroral zone in the summer hemisphere than occurred at solar minimum because of the larger heating rates during solar maximum. Again, there is an opposite variation between O and O_2 and N_2 similar to that obtained during solar minimum.

The calculated distributions of NO and N(^{4}S) number densities are shown in Figs 4a and 4b, respectively. Both species peak in the summer hemisphere and have a latitudinal distribution that decreases toward the winter hemisphere. Enhancement caused by auroral particle precipitation is evident in magnetic conjugate auroral zones. Maximum NO densities occur in the winter hemisphere lower thermosphere and are consistent with previous studies by Solomon *et al.* (1982) and Garcia *et al.* (1984) that indicate a downward transport of NO through the winter polar night region toward the stratosphere. The NO and N(^{4}S) densities calculated for solar maximum are somewhat larger than those calculated for solar minimum, shown in Fig. 3 of Paper I. These enhancements stem directly

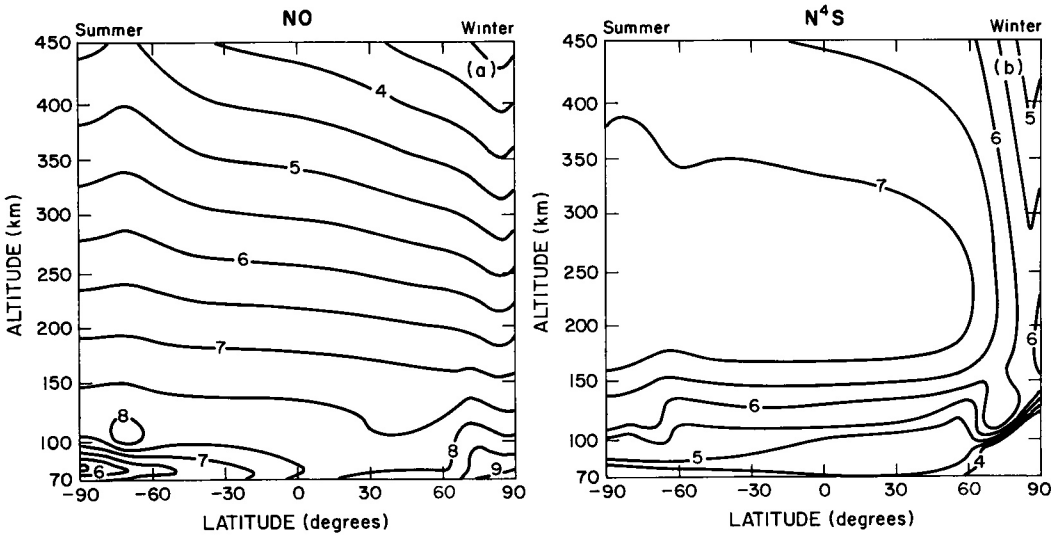

FIG. 4. CALCULATED ZONALLY AVERAGED DISTRIBUTION OF THE $\log_{10}$ (a) NO AND (b) N(^{4}S) NUMBER DENSITIES (cm^{-3}) FOR DECEMBER SOLSTICE AND SOLAR CYCLE MAXIMUM CONDITIONS FOR THE CASE WHEN NO COOLING IS INCLUDED.

or indirectly from the larger solar activity. In the upper thermosphere, where the nitric oxide density is directly controlled by temperature and molecular oxygen, the NO increase is a consequence of enhanced T and O_2. Near 110 km at low- and mid-latitudes, calculated densities are about twice as large as solar minimum values as a result of the increased ionization and dissociation due to the larger solar e.u.v. fluxes. At high latitudes, the NO peak is nearly unchanged since, due to the lack of knowledge of the solar cycle–particle flux dependence, the ionization rate by energetic particles was kept constant at its solar minimum value. Figure 5 illustrates the latitudinal distribution

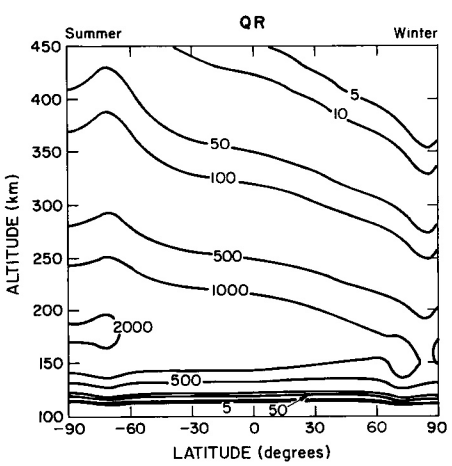

FIG. 5. LATITUDINAL DISTRIBUTION OF CALCULATED ZONALLY AVERAGED NO COOLING RATE IN K DAY^{-1} FOR DECEMBER SOLSTICE AND SOLAR CYCLE MAXIMUM CONDITIONS.

of the NO 5.3 μm cooling rate calculated with Kockarts' (1980) formulation and the temperature and number density fields displayed in Figs 2, 3 and 4. The larger value of the temperature in the thermosphere, combined with the enhanced NO density (itself resulting from the larger thermospheric temperature), accounts for the 4-fold increase of the peak of the cooling rate in comparison to the solar minimum situation. As in Paper I, the maximum is located between 150 and 180 km.

3.2. *Difference fields*

A model run identical to that described in the previous subsection, 3.1, was made without the NO cooling and difference fields were constructed. The model grid is on constant pressure surfaces so that interpretation is necessary to present the results on a constant height grid. Difference fields are constructed from solutions of model runs without NO cooling minus a model run with NO cooling. The calculated neutral gas temperature difference field is shown in Fig. 6a. The summer-to-winter pole exospheric temperature difference is weakened by about 110 K when NO cooling is included in the model. The temperatures decrease in the summer hemisphere and increase in the winter hemisphere from the case with no NO cooling is considered. This global response is caused by both radiative NO cooling and a weakened mean meridional circulation.

The weakened meridional temperature gradient for the case with NO cooling reduces the strength of the

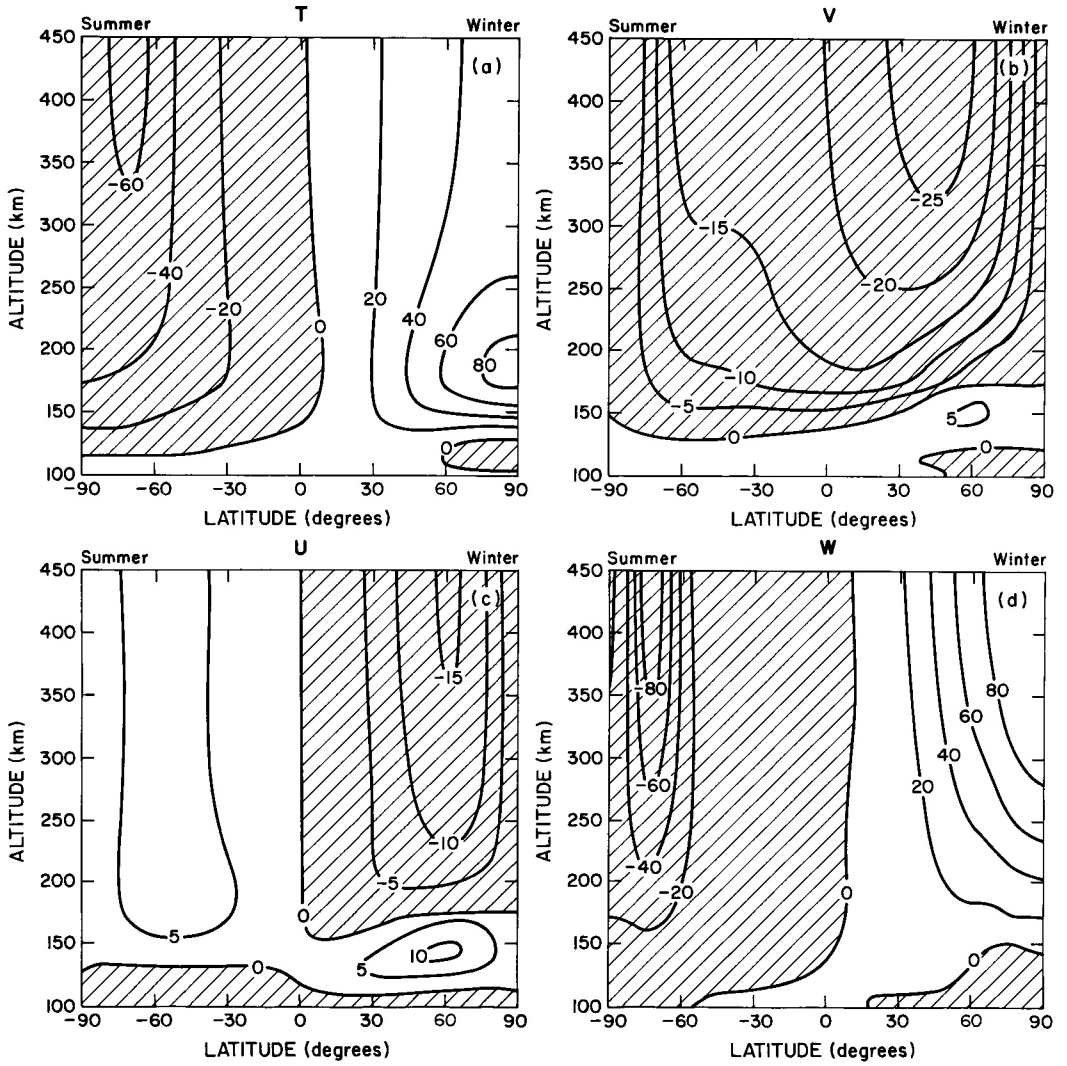

FIG. 6. LATITUDINAL DISTRIBUTION OF DIFFERENCE FIELDS BETWEEN MODEL RUNS (WITHOUT NITRIC OXIDE COOLING MINUS WITH NITRIC OXIDE COOLING) (a) TEMPERATURE DIFFERENCE (K), (b) ZONALLY AVERAGED MERIDIONAL WIND (m s^{-1}), (c) ZONALLY AVERAGED ZONAL WIND (m s^{-1}) AND (d) ZONALLY AVERAGED VERTICAL WIND (cm s^{-1}) FOR DECEMBER AND SOLSTICE DURING SOLAR MAXIMUM CONDITIONS.

mean meridional circulation as shown in Fig. 6b. There is a general weakening of the winds throughout the thermosphere with maximum values of about 25 m s^{-1} occurring at high mid-latitudes in the winter hemisphere. Below about 150 km, there is also a weakening of the return flow from the winter-to-summer hemisphere.

Zonal averaged zonal winds are also reduced as a result of the weakened meridional circulation as shown in Fig. 6c. In general, the changes in the zonal wind are less than 15 m s^{-1}.

The vertical winds are likewise as shown in Fig. 6d. Vertical wind velocity reductions are generally small (< 1 m s^{-1}) and are in a sense that reduces the mean meridional circulation. The overall effect of NO cooling during solar cycle maximum is to reduce the summer-to-winter hemisphere temperature gradient and mean meridional winds that in turn are associated with a weakening of zonal and vertical wind velocities and gradients in the mean compositional structure of the thermosphere. The percent changes in the difference of composition of the major constituents are shown in Fig. 7. Both N_2 and O_2 number densities are decreased in the summer hemisphere and enhanced in

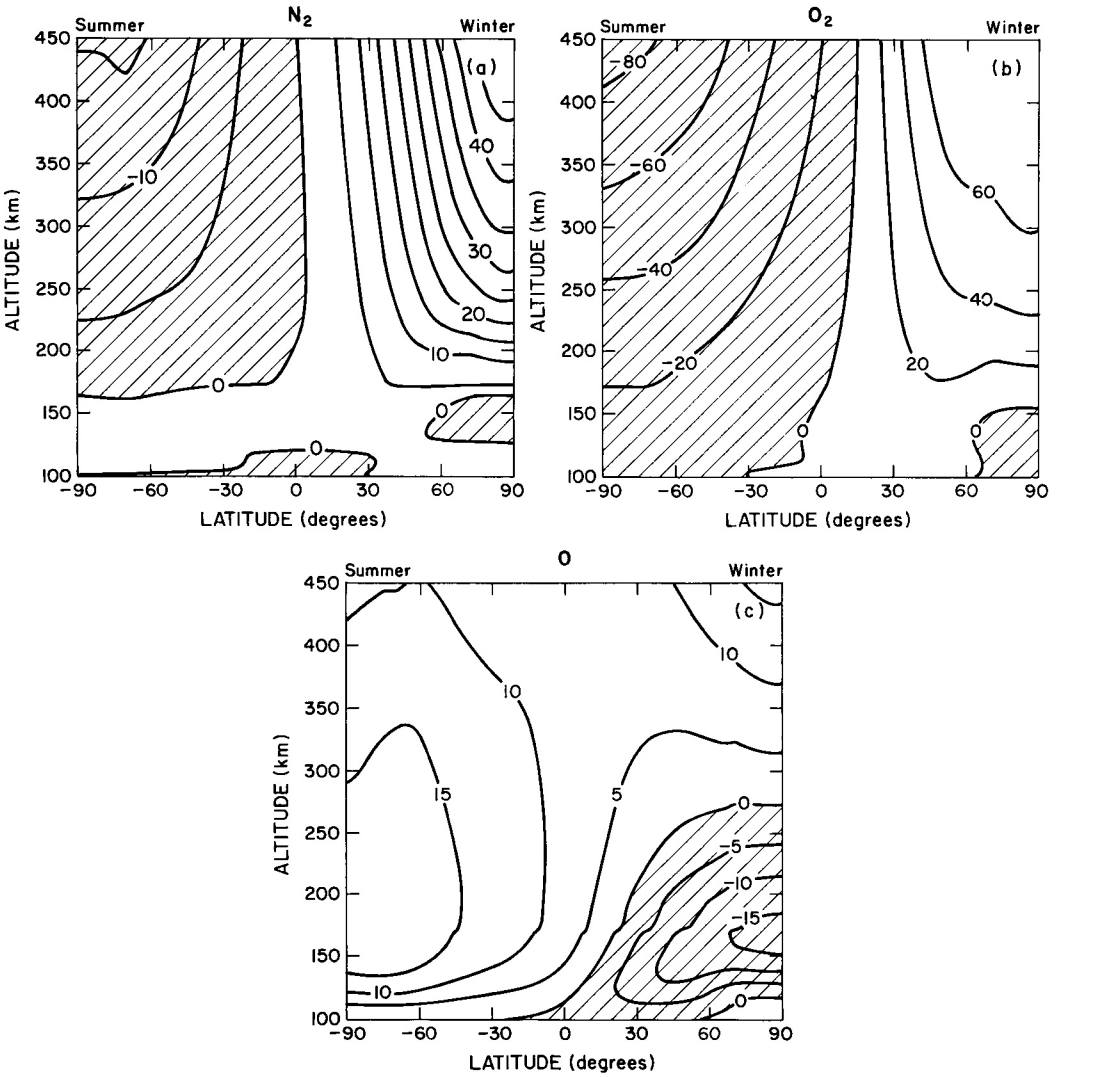

FIG. 7. SAME AS FIG. 5 EXCEPT FOR PERCENTAGE DIFFERENCE OF (a) N_2, (b) O_2 AND (c) O NUMBER DENSITIES (cm^{-3}).

the winter hemisphere as a result of the weakened mean meridional circulation. Atomic oxygen densities on the other hand are only weakly altered because of the compensating effects of weakened meridional circulation and colder thermospheric temperatures. Maximum variations occur in the lower thermosphere being +15% in the summer near 200 km and −15% near 150 km in the winter hemisphere. These calculations show that NO cooling has a more important role in establishing the mean circulation, temperature and compositional structure in the thermosphere for solar maximum than for solar minimum.

3.3. *Comparisons with MSIS*-83

The model calculations of perturbation temperature, N_2, O_2 and O number densities for December solstice conditions for solar maximum that are calculated with NO cooling and shown in Figs 2a, 3a, 3b and 3c, respectively, are now compared with MSIS-83 predictions shown in Fig. 8. The outputs from the MSIS-83 empirical model are shown for December solstice, $F_{10.7} = 200$, $A_p = 10$ and diurnally averaged conditions. The latitudinal distributions of perturbation temperature are similar for the two models. The calculated summer-to-winter pole exospheric

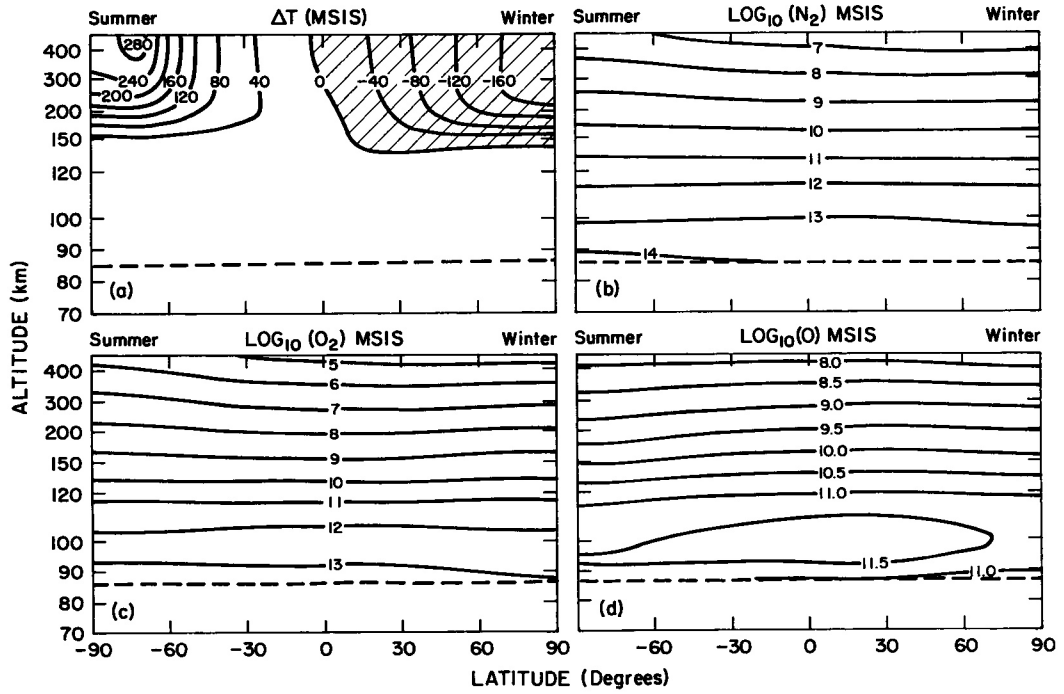

FIG. 8. ZONALLY AVERAGED (a) PERTURBATION TEMPERATURE (K), AND LOG_{10} NUMBER DENSITY DISTRIBUTIONS FOR (b) N_2, (c) O_2 AND (d) O OBTAINED FROM THE MSIS-83 EMPIRICAL MODEL OF TEMPERATURE AND COMPOSITION FOR DECEMBER SOLSTICE CONDITIONS AND SOLAR MAXIMUM CONDITIONS ($F_{10.7} = 200$, $A_p = 10$).

temperature difference is about 400 K whereas the MSIS-83 model predicts 440 K. This small difference is possibly linked in part to the choice of the electric field used at high latitudes in the two-dimensional model and the magnitude of the Joule heating source associated with this field. Both N_2 and O_2 number densities are enhanced in the summer hemisphere for the two models whereas O is enhanced in the winter hemisphere. There is general agreement between the calculated temperature and compositional structure and that predicted by the MSIS-83.

4. CONCLUSIONS

A zonally averaged chemical-dynamical model of the Earth's thermosphere has been used to investigate the importance of nitric oxide 5.3 μm cooling in controlling the overall structure and dynamics for December solstice conditions during solar maximum. The results were also compared with previous predictions made in Paper I for solar minimum and also with the temperature and composition structure in the MSIS-83 model. The results show that NO cooling for solar maximum is more important in controlling the overall structure of the thermosphere than for solar minimum. This occurs primarily because of the larger NO densities and thermospheric temperatures during solar maximum. In the upper thermosphere, NO 5.3 μm cooling reduced the summer-to-winter pole temperature difference by about 110 K with a 25 m s^{-1} reduction in the zonally averaged meridional wind speed. This compares to 45 K and 8 m s^{-1} for solar minimum. There are likewise larger reductions in the zonal and vertical wind speeds.

Acknowledgements—One of the authors (J.-C. G.) is supported by the Belgian Foundation for Scientific Research (FNRS). This work was supported in part by NATO Cooperative Research Grant No. 166/84 and by a FNRS grant. We acknowledge the National Center for Atmospheric Research for computing time. NCAR is sponsored by the National Science Foundation.

REFERENCES

Dickinson, R. E., Ridley, E. C. and Roble, R. G. (1975) Meridional circulation in the thermosphere, I. Equinox conditions. *J. atmos. Sci.* **32**, 1737.

Garcia, R. R., Solomon, S., Roble, R. G. and Rusch, D. W. (1984) A numerical response of the middle atmosphere to the 11-year solar cycle. *Planet. Space Sci.* **32**, 411.

Gérard, J. C. and Roble, R. G. (1986) The role of nitric oxide on the zonally averaged structure of the thermosphere:

solstice conditions for solar cycle minimum. *Planet. Space Sci.* **34**, 131.

Gérard, J. C., Roble, R. G., Rusch, D. W. and Stewart, A. I. (1984) The global distribution of thermospheric odd nitrogen for solstice conditions during solar cycle minimum. *J. geophys. Res.* **89**, 1725.

Hedin, A. E. (1983) A revised thermospheric model based on mass spectrometer and incoherent scatter data : MSIS-83. *J. geophys. Res.* **88**, 10170.

Kasting, J. F. and Roble, R. G. (1981) A zonally-averaged chemical-dynamical model of the lower thermosphere. *J. geophys. Res.* **86**, 9641.

Kockarts, G. (1980) Nitric oxide cooling in the terrestrial atmosphere. *Geophys. Res. Lett.* **7**, 137.

Roble, R. G. and Emery, B. A. (1983) On the global mean temperature of the thermosphere. *Planet. Space Sci.* **31**, 597.

Roble, R. G. and Kasting, J. F. (1984) The zonally averaged circulation, temperature, and compositional structure of the lower thermosphere and variations with geomagnetic activity. *J. geophys. Res.* **89**, 1711.

Rottman, G. J. (1981) Rocket measurements of the solar spectral irradiance during solar minimum, 1972–1977. *J. geophys. Res.* **86**, 6697.

Solomon, S., Crutzen, P. J. and Roble, R. G. (1982) Photochemical coupling between the thermosphere and the lower atmosphere, 1, Odd nitrogen from 50 to 120 km. *J. geophys. Res.* **87**, 7206.

Torr, M. R. and Torr, D. G. (1985) Ionization frequencies for solar cycle 21 : Revised. *J. geophys. Res.* **90**, 6675.

Torr, M. R., Torr, D. G. and Hinteregger, H. E. (1980) Solar flux variability in the Schumann–Runge continuum as a function of solar cycle 21. *J. geophys. Res.* **85**, 6063.